PERSPECTIVE

NJC
www.rsc.org/njc

Chemical modification of C_{60} for materials science applications†

Jean-François Nierengarten

Groupe de Chimie des Fullerènes et des Systèmes Conjugués, Ecole Européenne de Chimie, Polymères et Matériaux, Université Louis Pasteur et CNRS, 25 rue Becquerel, 67087 Strasbourg cedex 2, France. E-mail: jfnierengarten@chimie.u-strasbg.fr

Received (in Montpellier, France) 18th February 2004, Accepted 30th March 2004
First published as an Advance Article on the web 1st September 2004

Fullerene derivatives have shown a wide range of physical and chemical properties that make them attractive for the preparation of supramolecular assemblies and new materials. As a part of this research, we are interested in the chemical modification of C_{60} for various applications. These results are summarized in the present account to illustrate the current state-of-the-art of fullerene chemistry for the development of new advanced materials. In the first part, some of the fundamental architectural requirements needed for the design of amphiphilic fullerene derivatives capable of forming stable Langmuir films are reported. In particular, we have shown that the encapsulation of C_{60} in a cyclic addend surrounded by long alkyl chains, cholesterol subunits or dendritic branches is an efficient strategy to prevent the irreversible aggregation resulting from the strong fullerene-fullerene interactions usually observed for amphiphilic C_{60} derivatives at the air–water interface. In the second part, water-soluble C_{60} derivatives and fullerene-functionalized dendrimers are described. These compounds are easy to process, owing to their high solubility, and thus easily incorporated in mesoporous silica glasses for optical limiting applications. Finally, our recent developments on organic photovoltaic cells using covalently linked fullerene-(π-conjugated oligomer) ensembles as the active layer are summarized. This molecular approach appears to be particularly interesting since the behavior of a unique molecule in a photovoltaic cell and the study of its electronic properties means one can easily obtain the structure-activity relationships leading to a better understanding of the photovoltaic conversion.

Introduction

Since C_{60} became available in macroscopic quantities in 1990,[1] the physical properties of this fascinating carbon cage have been intensively investigated. Among the most spectacular findings, C_{60} was found to behave like an electronegative molecule able to reversibly accept up to six electrons,[2] to become a supraconductor in M_3C_{60} species (M = alkali metals)[3] or to be an interesting material with non-linear optical properties.[4] However, this new molecular material aggregates very easily and is insoluble or only sparingly soluble in most solvents.[5] Therefore, pristine C_{60} is difficult to handle. This serious obstacle for practical applications can be, at least in part, overcome with the help of organic modifications of C_{60}. Effectively, the recent developments in the functionalization of fullerenes allow the preparation of highly soluble C_{60} derivatives easier to handle; the electronic properties, such as facile multiple reducibility, optical non-linearity or efficient photosensitization, that are characteristic of the parent fullerene are maintained for most of the C_{60} derivatives.[6] As a part of this research, we became interested in the chemical modification of C_{60} for various applications in materials science. Some of these results are summarized in the present account to illustrate our current understanding of the structure-activity relationships and molecular engineering of fullerene derivatives for the development of new advanced materials.

Jean-François Nierengarten was born in Strasbourg, France, in 1966. He studied biochemistry and chemistry at the Université Louis Pasteur of Strasbourg, France, and received his doctoral degree under the supervision of Jean-Pierre Sauvage and Christiane Dietrich-Buchecker in Strasbourg in 1994. After postdoctoral work with François Diederich at the ETH-Zürich, Switzerland, during 1994–1996, he returned to Strasbourg as a CNRS researcher. His current scientific interests range from covalent chemistry of fullerenes to dendrimers and π-conjugated systems with unusual electronic and optical properties.

† Dedicated to the memory of Professor Jean-Marc Kern. He passed away in the tragic airplane accident over Sharm el-Sheikh on the 3rd of January, 2004.

Amphiphilic C_{60} derivatives and their incorporation in Langmuir and Langmuir–Blodgett films

Since the incorporation of fullerenes into thin films is required for the preparation of many optoelectronic devices, the past several years have seen a considerable growth in the use of fullerene-based derivatives at surfaces and interfaces.[7] One possible approach towards structurally ordered fullerene assemblies is the preparation of Langmuir films at the air–water interface and their subsequent transfer onto solid substrates.[7] However, all the studies on the spreading behavior of pure fullerenes at the air–water interface revealed the formation of collapsed films due to the non-amphiphilic nature of these compounds and to aggregation phenomena resulting from strong fullerene-fullerene interactions.[8] Furthermore, all attempts to create well-defined Langmuir–Blodgett (LB) films have failed.

DOI: 10.1039/b402661f

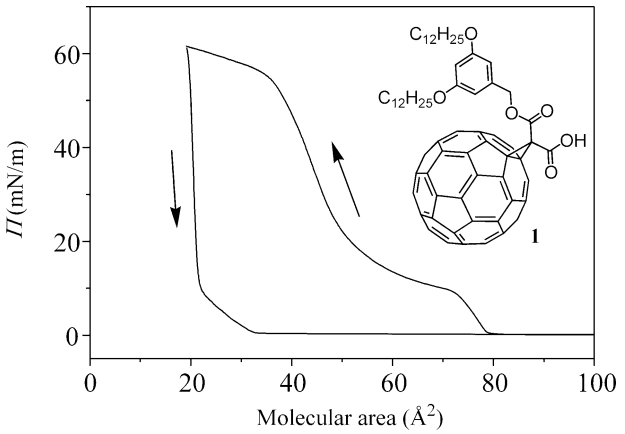

Fig. 1 Hysteresis curve of the Π–A isotherm, showing the irreversibility of the isotherm of **1**.

Two approaches have been used to overcome these problems. The first one consists in preventing the fullerene-fullerene interactions by incorporating the fullerenes into a matrix of an amphiphilic compound to produce mixed Langmuir films. Fatty acids or long-chain alcohols have been used for this purpose;[9] however, the expected protection is not always very effective and fullerene aggregation remains a problem. Amphiphilic molecules containing a cavity able to incorporate the fullerene, such as azacrowns[10] or calixarenes,[11] have been found to be the most suitable matrices for the preparation of fullerene-containing composite Langmuir films of good quality. The second approach is achieved by chemical modification of the fullerene molecule, in general by covalent attachment of a hydrophilic head group onto the fullerene core to obtain an adduct with an amphiphilic character.[12,13] By attaching a hydrophilic head group to the fullerene core, significant improvement of the spreading behavior has been reported. The polar head group is responsible for an attractive interaction with the aqueous subphase, thus preventing three-dimensional aggregation and allowing the preparation of monolayers at the air–water interface. However, in most of the cases, once the fullerene cores are in contact with each other in the compressed Langmuir films, they irreversibly aggregate and the monolayer no longer expands back to the initial state. The resulting Langmuir films are also usually rigid and, as a result, their transfer onto solid substrates is difficult. As part of this research, we have decided to prepare a compound combining the advantages of these two approaches, meaning a C_{60} derivative substituted at the same time with a polar head group (to obtain an adduct with an amphiphilic character) and long alkyl chains (to prevent the fullerene-fullerene interactions).[14] Therefore, compound **1** was synthesized[14,15] and its Π–A isotherm is depicted in Fig. 1.

Even if compound **1** behaves slightly better than pure C_{60}, a strong tendency to escape from the air–water interface to form three-dimensional aggregates is observed. Effectively, the molecular area extrapolated to zero surface pressure is $A_0 \approx 80$ Å^2, which is obviously too small for such a molecule, and Brewster angle microscopy (BAM) observations of the films obtained from **1** revealed the presence of defects in the structure.[14] In addition, once the fullerene cores are in contact with each other, they irreversibly aggregate and the layer no longer expands back. It appears that the expected protection resulting from the presence of the two long alkyl chains is not efficient enough and fullerene aggregation still occurs. In order to improve the spreading behavior of the amphiphilic fullerene derivatives, two additional long alkyl chains were attached to the C_{60} sphere, leading to **2**–**5** (Chart 1).[14,16,17] In the design of these compounds, it is worth noting that a cyclic structure was chosen in order to encapsulate the fullerene core in its addend and thus to prevent more efficiently the aggregation observed with other amphiphilic C_{60} derivatives such as **1**.

As a typical example, the Π–A isotherm obtained with **2a** is shown in Fig. 2. The surface pressure rises to around $A \approx 145$ Å^2 and the molecular area extrapolated at zero surface pressure is $A_0 \approx 136$ Å^2, in good agreement with the value that can be estimated by molecular modeling. These films show excellent reversibility if Π is kept below the collapse pressure, $\Pi_c \approx 18$ mN m^{-1}. The latter observation clearly indicates that the four alkyl chains are able to efficiently prevent the aggregation resulting from fullerene-fullerene interactions. BAM observations show that the film obtained from **2a** is non-continuous at large molecular areas, with holes through which water can be seen (Fig. 2).[16] These small circular domains shrink and disappear when the surface pressure reaches $\Pi \approx 10$ mN m^{-1} and as long as the film does not enter the collapse regime, only homogeneous surfaces are observed. Compounds **2b** and **2c**, respectively the $C_{12}H_{25}$ and $C_{16}H_{33}$ analogs of **2a**, also form good quality Langmuir films, with collapse pressures

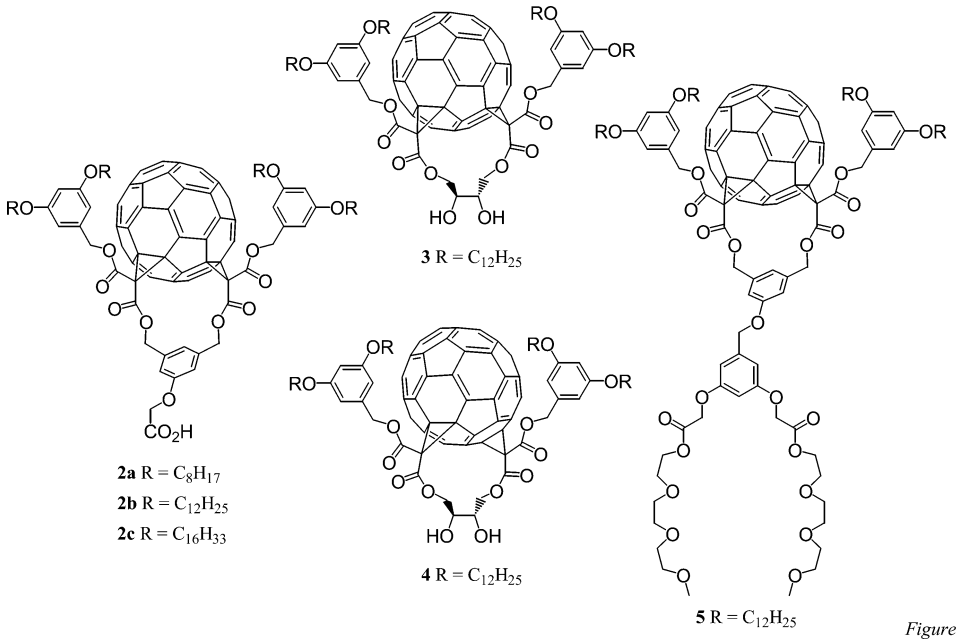

Figure 2

Chart 1 Amphiphilic fullerene derivatives **2**–**5**.

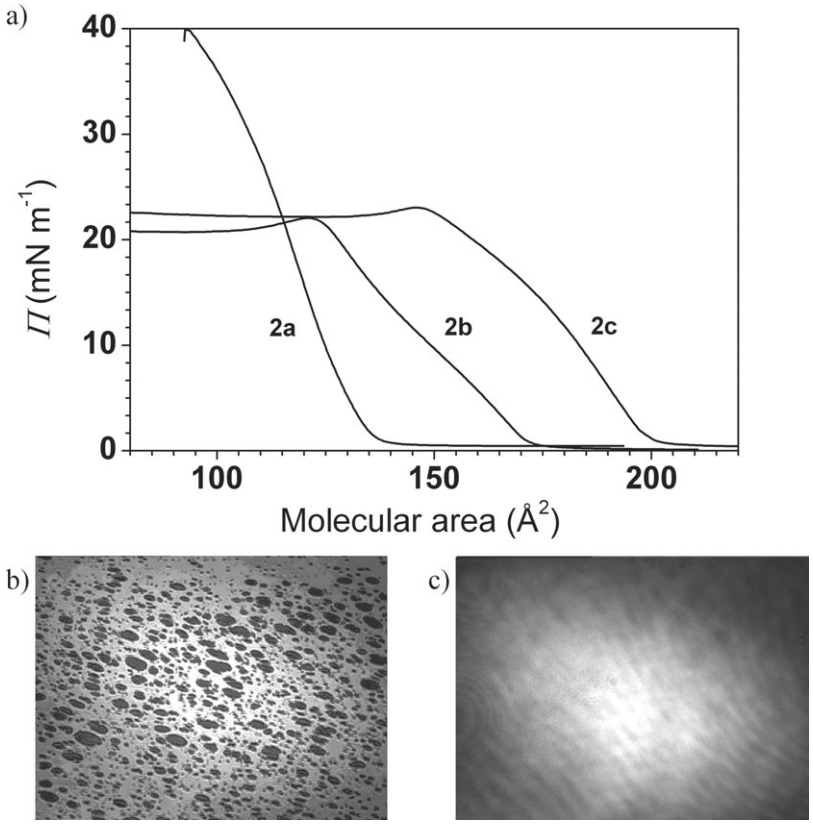

Fig. 2 (a) Pressure-area isotherms for **2a**, **2b** and **2c**. (b) Brewster angle microscopy image for **2a** at $A = 180$ Å^2. (c) Brewster angle microscopy image for **2a** at $A = 135$ Å^2.

around 20 mN m^{-1} (Fig. 2). However, upon compression, **2b** and **2c** exhibit a somewhat different behavior when compared to **2a**.[17] Effectively, the pressure levels off and becomes almost independent of the molecular area. Actually, when the chain length is increased, the hydrophobic-hydrophilic balance becomes less favorable and, as a result, the molecules are easier to expel from the surface. It is also interesting to notice the values obtained for the molecular area extrapolated at zero surface pressure as a function of the chain length: $A_0 \approx 136$ (C_8H_{17}), 170 ($C_{12}H_{25}$), and 204 ($C_{16}H_{33}$) Å^2. This increase of the extrapolated molecular area with the chain length indicates that the chains are not perpendicular to the water surface.

The Π–A isotherms of compounds **3**–**4** are very similar to that of **2b**.[17] The films also show excellent reversibility upon successive compression/decompression cycles as long as the collapse pressure is not exceeded; the BAM pictures at the end of the compression look exactly like that depicted in Fig. 2 for **2a**. The molecular area extrapolated at zero pressure and the collapse pressure being the same for **2b**, **3** and **4**, the hydrophilic-hydrophobic balance and the anchoring on the water surface must be similar for these three compounds. For compound **5** with two triethylene glycol units and $C_{12}H_{25}$ chains, a sizeable increase of the collapse pressure is observed when compared to the $C_{12}H_{25}$ analogs **2b**, **3** and **4** described above, indicating a more favorable hydrophilic-hydrophobic balance and a better anchoring of the molecules on the water surface.[17] The isotherm shows a nice behavior: the surface pressure starts to increase smoothly at $A \approx 140$ Å^2 until collapse, which occurs at $\Pi_c \approx 40$ mN m^{-1} (Fig. 3). Here again, the behavior is reversible if Π_c is not exceeded. A closer look at the shape of the various isotherms reveals that for the compounds with a small polar head group, the surface pressure started to increase steadily at some point, with an almost constant compressibility, whereas in the case of **5** there is a first regime between $A \approx 145$ and 110 Å^2 where the compressibility gradually increases before remaining constant. The molecular area extrapolated at zero pressure is $A_0 \approx 120$ Å^2. When compared to **2b**, **3** and **4** for which $A_0 \approx 170$ Å^2, the lower value obtained for **5** points to a higher film density, hence a better molecular packing. We believe that this smaller A_0 value and the observation of a liquid expanded phase between 145 and 110 Å^2 must result from the better anchoring of **5** when compared to analogous compounds with a smaller polar head group. Effectively, since the molecules are not easily expelled from the water surface at high pressure, they are forced to adopt a compact conformation in which the long alkyl chains are pushed perpendicular to the water surface.

In collaboration with the group of Deschenaux,[18] we have also shown that substitution of the amphiphilic cyclic fullerene bisadduct substructure with cholesterol groups is a convenient way for the preparation of suitable derivatives for efficient incorporation in Langmuir films. The amphiphilic fullerene bisadducts **6** and **7** substituted with two and four cholesterol residues, respectively, have been prepared (Chart 2). Whereas homogeneous Langmuir films have been obtained for both **6**

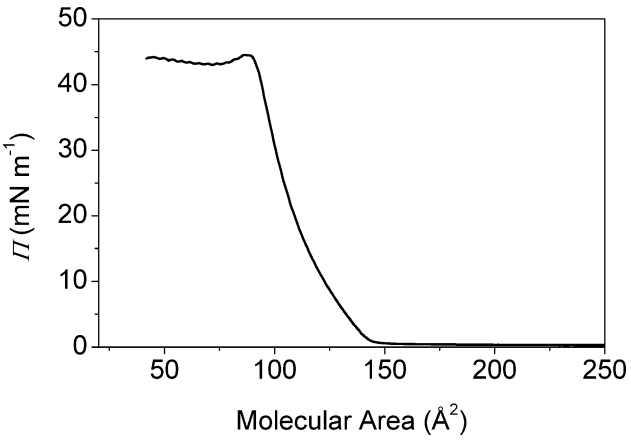

Fig. 3 Pressure-area isotherm for **5**.

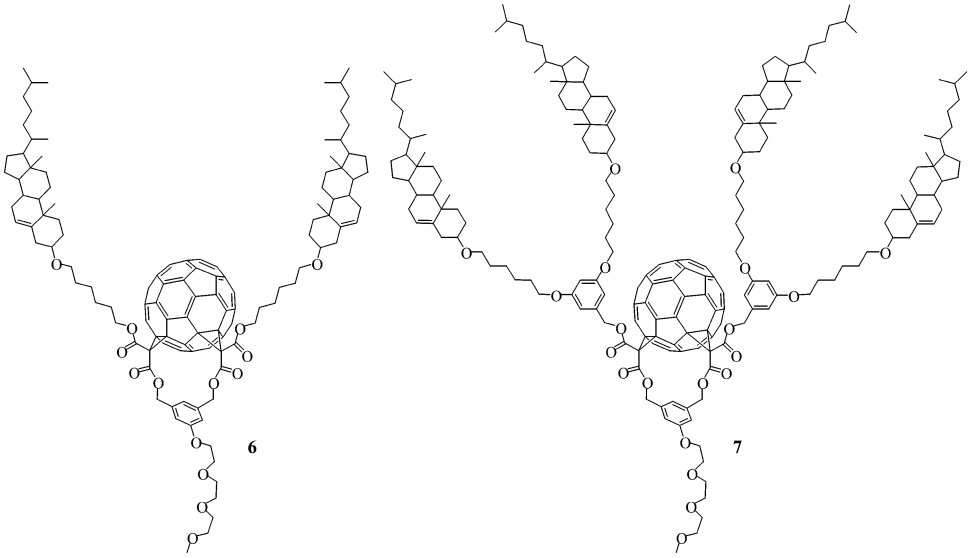

Chart 2 Amphiphilic fullerene derivatives **6** and **7**.

and **7**, only the films obtained with **7** show a reversible compression-expansion behavior. This suggests that by increasing the number of cholesterol subunits, the encapsulation of the carbon sphere in its addend is more efficient, thus limiting fullerene-fullerene interactions and aggregation phenomena.

The Langmuir films obtained from the amphiphilic fullerene bisadducts **2**–**7** have been transferred onto solid substrates with the LB technique.[17,18] A great number of layers could be deposited without any problem. The excellent quality of the LB films prepared with these amphiphilic fullerene bisadducts is deduced from the plot of their UV/Vis absorbance as a function of the layer number, which results in straight lines, indicating an efficient stacking of the layers. The main feature of the UV/Vis spectra is the broadening of the absorption in the LB films when compared to the solution.[17] The latter observation is indicative of fullerene-fullerene interactions within the LB films. Due to the presence of the long alkyl chains around the C_{60} subunits within a layer, we believe that these fullerene-fullerene interactions may be the result of the contact of carbon spheres from neighboring layers rather than within the layers. The structural quality of the LB films was also probed by grazing incidence X-ray diffraction measurements.[16] In the case of **2a**, we have shown that the molecules of even layers do not deposit atop odd ones, but partially wedge themselves in-between, like hard spheres piling up on hard

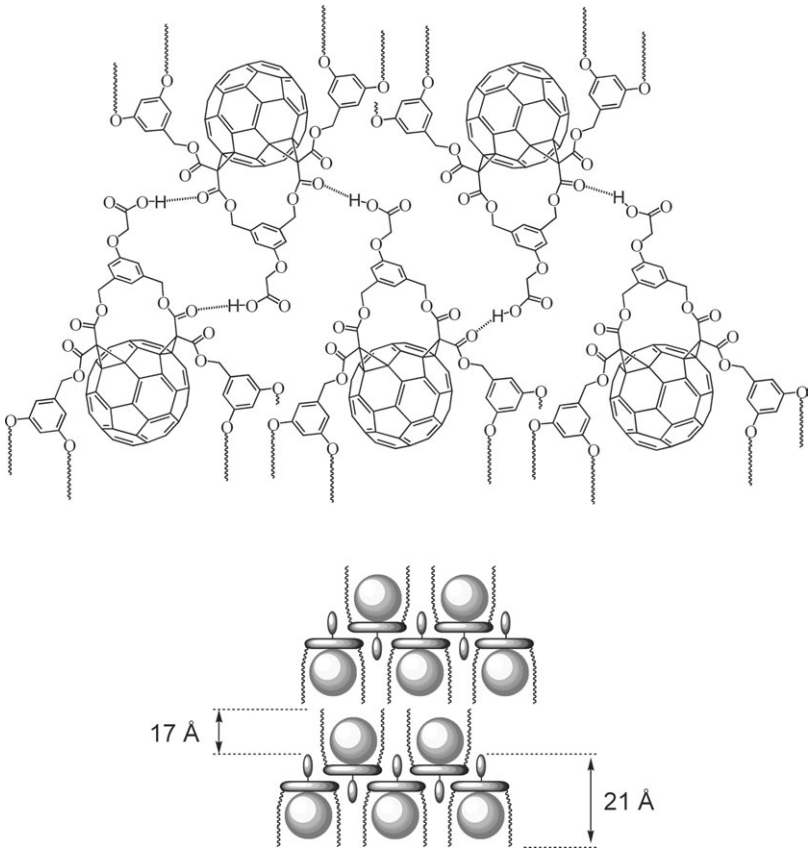

Fig. 4 Schematic model of the structure of the multilayer LB films obtained from **2a**.

spheres (Fig. 4). Molecular modeling shows that this model is indeed reasonable and suggests that intermolecular hydrogen bonds could take place, as schematically depicted in Fig. 4, providing additional stabilization of the films. The IR spectra of the multilayer films of **2a** showing a signal at 3340 cm^{-1} are in good agreement with the presence of such hydrogen bonds.

The encapsulation of a fullerene moiety in the middle of a dendritic structure is another efficient strategy to obtain amphiphilic derivatives with good spreading characteristics.[19,20] Effectively, the functionalization of C_{60} with a controlled number of dendrons provides a compact insulating layer around the carbon sphere, capable of preventing contact between neighboring fullerenes when the film is compressed; thus, the irreversible aggregation usually observed for amphiphilic fullerene derivatives cannot occur. As part of this research, we have recently reported the synthesis of diblock globular fullerodendrimers **8**–**10** with hydrophobic chains on one hemisphere and hydrophilic groups on the other one (Chart 3).[21] Actually, the hydrophobic-hydrophilic balance of these dendrimers has been systematically modified by changing the size of the polar head group in order to investigate the role of the amphiphilicity at the air–water interface and during the deposition onto solid substrates.

Langmuir films have been obtained with dendrimers **8**–**10**. Regardless of its size, the polar head group of these compounds is responsible for an attractive interaction with the aqueous subphase, thus forcing the molecules towards the water surface in a two-dimensional arrangement. The pressure-area (Π–A) isotherms of fullerodendrimers **8**–**10** are depicted in Fig. 5. The three compounds exhibit a similar behavior: the surface pressure Π increases smoothly at molecular areas between 400 and 500 $Å^2$ before taking a sharper rise between 250 and 350 $Å^2$, depending on the compound. The general shape of the isotherms indicates that the films are at first in a liquid-condensed

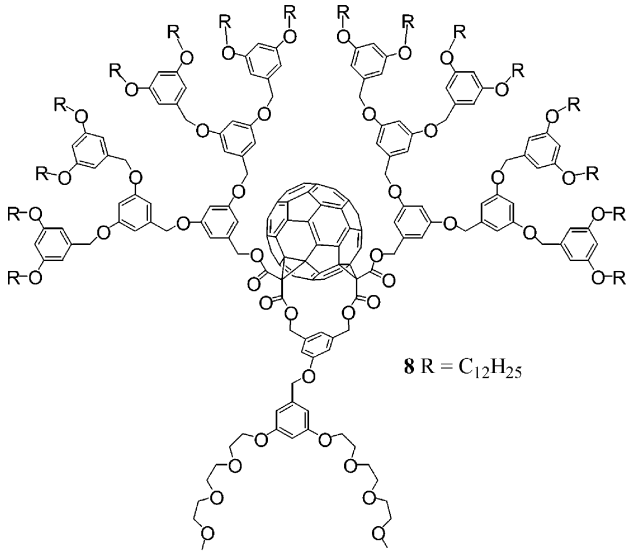

8 R = $C_{12}H_{25}$

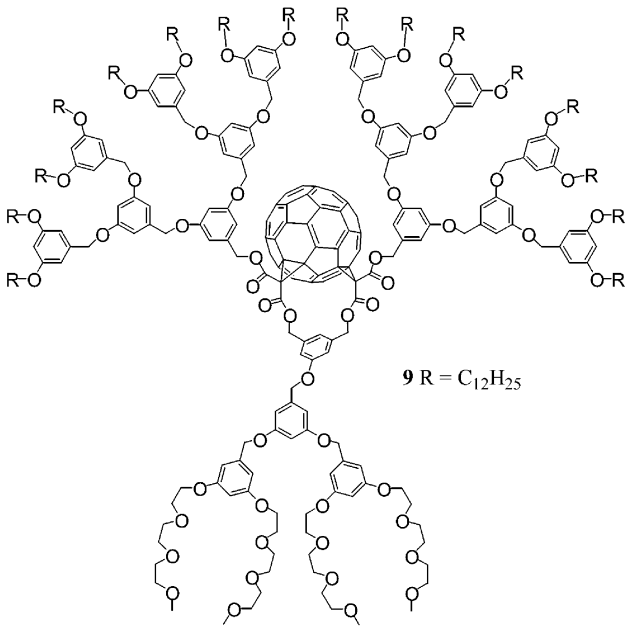

9 R = $C_{12}H_{25}$

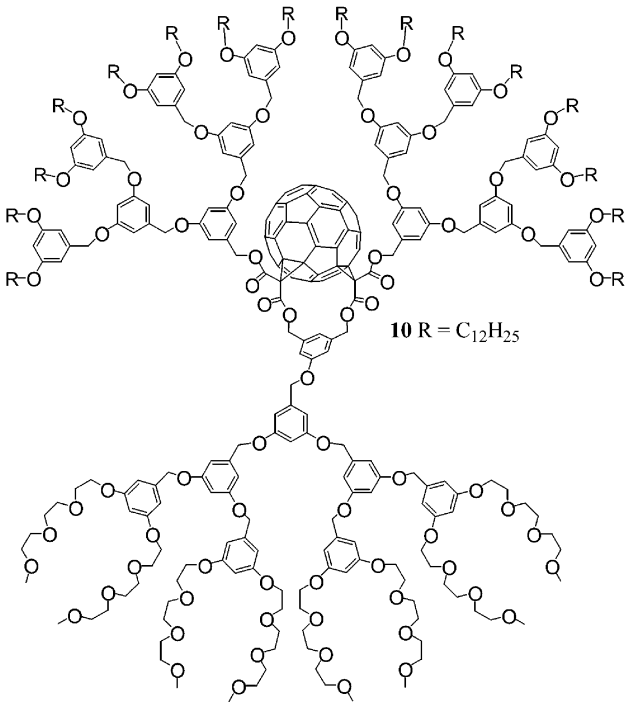

10 R = $C_{12}H_{25}$

Chart 3 Amphiphilic fullerene derivatives **8**–**10**.

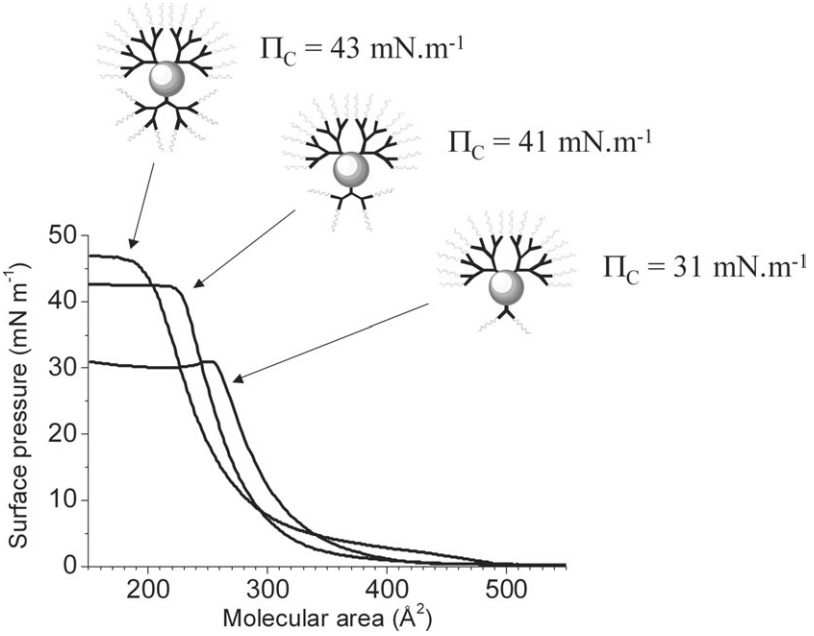

Fig. 5 Pressure-area isotherms of compounds **8**–**10** taken on pure water at 20 °C. The collapse pressure increases with the size of the polar head group.

phase. Final molecular areas A_0 extrapolated at zero surface pressure are 320 ± 3 (**8**), 295 ± 3 (**9**) and 280 ± 3 (**10**) Å^2, in good agreement with the value that can be estimated by molecular modeling. Interestingly, the A_0 values decrease as the size of the polar head group increases. The latter observation could be ascribed to a conformational change in the dendritic structure when the anchoring on the water surface is stronger. The repulsion of the $C_{12}H_{25}$ terminated dendrons from the water surface must be more effective in the case of **9** and **10** and, as a result, the molecules adopt a more compact structure. In other words, the two $C_{12}H_{25}$ terminated dendritic branches are forced to wrap the fullerene core. In contrast, for compound **8**, the dendritic structure may be less densely packed around the central fullerene core due to the weaker anchoring on the water surface. This model is further supported by observations on the LB films prepared from the Langmuir films of compounds **8**–**10** (see below).

Using the LB technique, it has been possible to transfer the Langmuir films made from **8**–**10** and to obtain multilayers on solid substrates. In accordance with previous observations, transfer is more efficient upon increasing the size of the polar head group. The excellent quality of the LB films prepared from these amphiphilic dendrimers is deduced from the plot of their UV/Vis absorbance as a function of the layer number, which results in straight lines, indicating that the films obtained from **8**–**10** grow regularly. As discussed above for the LB films prepared from **2**–**7**, the main feature of the UV/Vis spectrum of the LB film of **8** is the broadening of the absorption in the film when compared to the solution. The latter observation is indicative of fullerene-fullerene interactions resulting from contacts of carbon spheres among neighboring layers. Remarkably, a clear evolution can be seen by going from **8** to **10**: the broadening of the absorption spectrum seen for **8** has almost vanished for **9** and **10**. Actually, the UV/Vis spectra of LB films of **9** and **10** are close to the ones recorded in CH_2Cl_2 solutions, suggesting limited fullerene-fullerene interactions within the LB film. This observation is in full agreement with the more compact structures proposed for **9** and **10** at the air–water interface when compared to **8**. In summary, the Langmuir studies of fullerodendrimers **8**–**10** have revealed a conformational change in the dendritic structure with the size of the polar head group. Due to a better anchoring onto the water surface, the compounds with the largest polar head groups adopt a more compact structure and the dendritic branches are forced to wrap the fullerene core. This model is nicely confirmed by the extent of fullerene-fullerene interactions within the LB films as deduced from their absorption spectra. On the one hand, the results obtained in this systematic study show some of the fundamental architectural requirements for obtaining stable Langmuir films with amphiphilic dendrimers. On the other hand, it is worth noting that the fullerene chromophores are almost completely isolated from external contacts by the dendritic structure, thus paving the way toward ordered thin films of isolated functional molecular units. This appears to be an important finding for future nanotechnological applications, in particular for data storage at a molecular level.

C_{60} derivatives for optical limiting applications

Several studies on fullerene derivatives have shown the great potential of this class of materials for optical limiting applications.[4] Effectively, the transmission of fullerene solutions decreases by increasing the light intensity. For short pulses (ps), the limiting action is ascribed to pure reverse saturable absorption (RSA) whereas for longer pulses (ns–μs) additional mechanisms of mainly thermal origin are invoked.[22,23] Even if these solutions are efficient optical limiters, the use of solid devices is largely preferred for practical applications due to their greater ease of handling. Therefore, crystalline films of C_{60} have been studied, but found to be inefficient against pulses longer than tens of ps. This result is ascribed to a fast de-excitation of the laser-created excited state due to interactions of neighboring C_{60} molecules in the solid phase.[22] In contrast, it has been shown that C_{60} keeps its optical limiting properties after inclusion in solid matrices such as sol-gel glasses,[24] polymethyl methacrylate (PMMA) matrices[25] and glass-polymer composite samples.[26]

As far as sol-gel glasses are concerned, special procedures have to be employed since good solvents for fullerenes are incompatible with the sol-gel process.[22,27] Actually, incorporation of fullerenes is typically achieved by soaking mesoporous silica glasses with a solution of C_{60}.[24] In this context, we have shown that another efficient approach is to incorporate water-soluble C_{60} derivatives, compatible with the sol-gel process, directly into the sol.[28] For this purpose, water-soluble methanofullerene **11** was prepared (Fig. 6).[28] Successful inclusion of

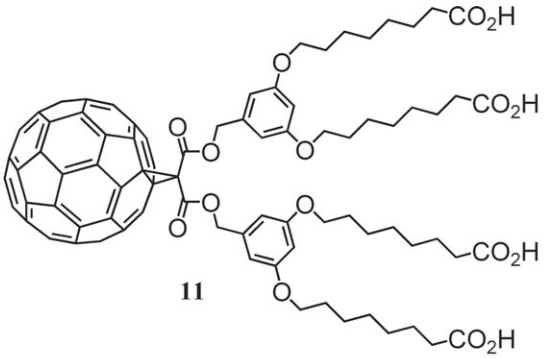

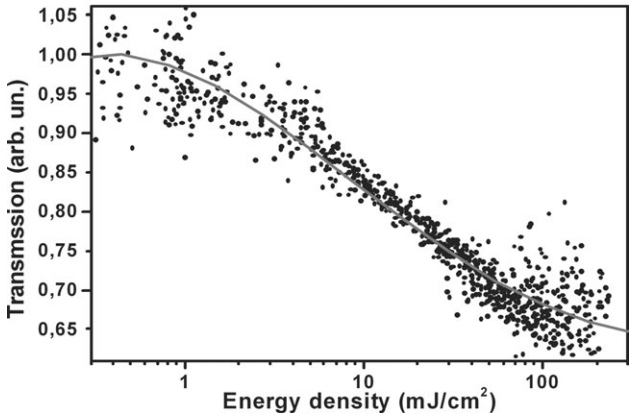

Fig. 6 Transmission *versus* incident fluence at 532 nm of a sol-gel sample containing compound **11**.

compound **11** in the sol-gel could effectively be achieved during the gelation process. A saturated solution of **11** in a 1 : 1 mixture of water and THF containing a small amount of ammonia was mixed quickly to the sol-gel preparation in the casting boxes. A few seconds after mixing, gelation occurred due to the pH change. The resulting dark red glasses were perfectly homogeneous and used as made for the optical measurements.

The transmission of the sample at 532 nm as a function of the incoming laser fluence is shown in Fig. 6. With increasing pulse energy, the transmission of the sample clearly decreases. The threshold for the onset of the limiting action is located at about 3 mJ cm^{-2}, a value comparable or even slightly lower than that obtained with inclusions of C_{60} in sol-gel matrices.[22] The damage threshold of our samples is about 200 mJ cm^{-2}. Up to this fluence, the effect is fully reversible. For higher values, we observe cumulative damage of the C_{60} molecules in their glass environment. With the same pulse lengths, the threshold value is considerably smaller than that of materials showing simultaneous two-photon absorption. Even among materials showing RSA, this value is quite good.[22] It is similar to the one found in C_{60} solutions, confirming the fact that C_{60} keeps its favorable limiting properties even after chemical modification. However, for sol-gel-glasses doped with plain C_{60} or methanofullerene **11**, faster de-excitation dynamics and reduced triplet yields are observed when compared to the solutions. The latter observations have been mainly explained by two factors: (i) perturbation of the molecular energy levels due to the interactions with the sol-gel matrix and (ii) interactions between neighboring fullerene spheres due to aggregation.[22,28]

In order to prevent such undesirable effects, we have prepared fullerodendrimers **12**–**13** (Chart 4) in which the C_{60} core is buried in the middle of a dendritic structure.[29–33] The incorporation of fullerodendrimers **12**–**13** in sol-gel glasses has been easily achieved by soaking mesoporous silica glasses with a solution of **12**–**13**.[30] The resulting samples only contain well-dispersed fullerodendrimer molecules. Preliminary measurements on the resulting doped samples have revealed efficient optical limiting properties.[30] The transmission as a function of the fluence of the laser pulses is shown in Fig. 7. It remains nearly constant for fluences lower than 5 mJ cm^{-2}. When the intensity increases above this threshold, the effect of

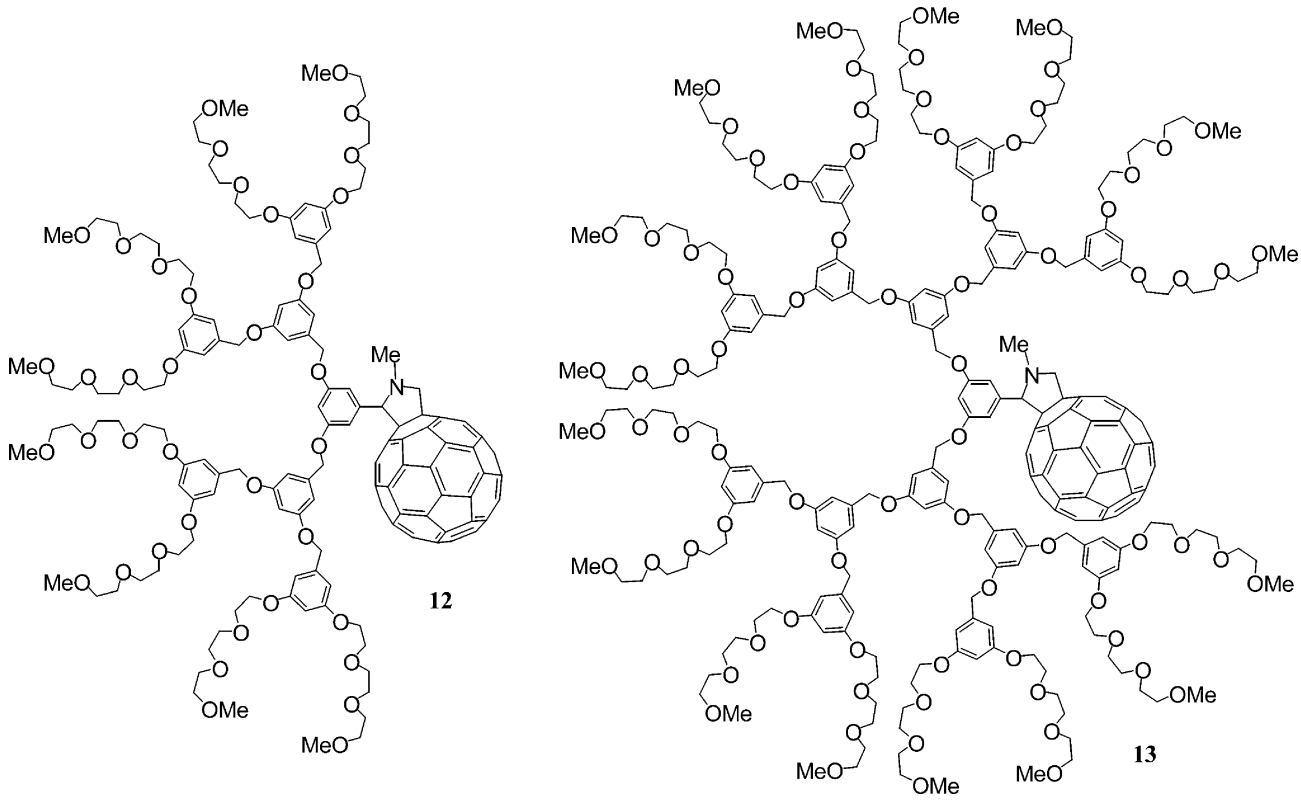

Chart 4 Fullerodendrimers **12** and **13**.

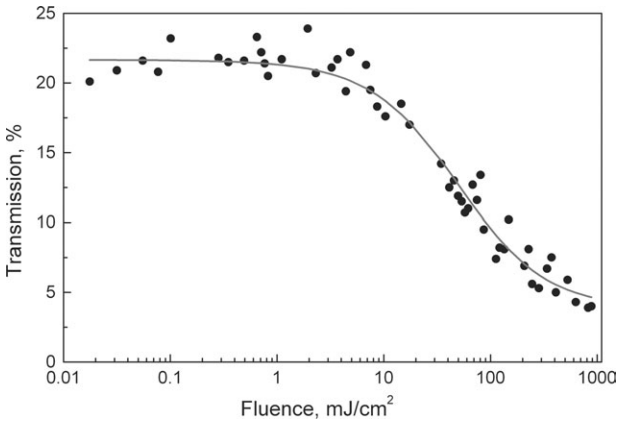

Fig. 7 Transmission *versus* incident fluence at 532 nm of a sol-gel sample containing compound **12**.

induced absorption appears and the transmission diminishes rapidly, thus showing the potential of these materials for optical limiting applications. Further studies are under way in order to determine the influence of the dendritic branches on the optical limiting behavior of these composite materials.

C_{60} derivatives for photovoltaic applications

Following the observation of ultrafast photoinduced electron transfer from conjugated polymers to C_{60},[34] a novel approach to the preparation of photovoltaic devices has been proposed by Heeger, Wudl and co-workers.[35] It is based on an interpenetrating blend of donor (conjugated polymer) and acceptor (C_{60}) sandwiched between two asymmetric contacts (two metals with different work functions). When the donor is excited, the electron promoted to the lowest unoccupied molecular orbital (LUMO) will lower its energy by moving to the LUMO of the acceptor. Under the influence of the inherent electric field caused by the asymmetric contacts, separation of the opposite charges takes place, with the holes being transported in the donor phase and the electrons in the acceptor. In this way, the blend can be considered as a network of donor-acceptor heterojunctions that allows efficient charge separation and balanced bipolar transport throughout its whole volume.[36] Remarkably, the efficiency of the bulk heterojunction devices consisting of poly[2-methoxy-5-(3,7-dimethyloctyloxy)]–*p*-phenylenevinylene (MDMO–PPV) and 1-(3-methoxycarbonyl)-propyl-1-1-phenyl-(6,6)C_{61} (PCBM) was increased to 3% by the group of Sariciftci.[37] However, for commercial use the efficiency and the stability of the organic photodiodes have to be improved dramatically. For these purposes π-conjugated polymers with a strong absorption in all the visible range and a good stability towards light are needed. Additionally, the initially formed phases between the donor and acceptor have to be fixed by either cross-linking the two compounds or using polymer-polymer mixtures with high T_g since the two phases tend to separate due to the operational heat through illumination, thus reducing progressively the performances of the device. This prompted us to start a research program on C_{60} functionalized macromolecules for the preparation of all-polymer solar cells.[38–39] The two major problems for the preparation of such polymers are the multifunctional character of C_{60} and its chemical reactivity typical of an electron-deficient olefin. Actually, radical and anionic polymerizations of fullerenes lead to star-shaped polymers with relatively low fullerene content and/or to non-processible cross-linked polymers.[40–41] The controlled incorporation of fullerenes into well-defined linear polymers can, however, be achieved by the side-chain functionalization of polymers[42] or by the polycondensation of bifunctional fullerene adducts with bifunctional reagents.[43] As part of this research, we have shown that the controlled incorporation of fullerenes into well-defined linear polymers can be achieved by polycondensation of the bifunctional fullerene derivative **14** with diols (Scheme 1).[38] The experimental conditions (temperature, concentration and reaction time) were optimized to improve the yields and to obtain polymers with the highest molecular weight. At the end of the polymerization reaction, the resulting THF solution was poured into methanol to precipitate the polymer. Purification by preparative size exclusion chromatography (SEC) to remove the low molecular weight materials then afforded the polymer **15** in 60% yield as a dark red glassy compound.

Polymer **15** is well-soluble in common organic solvents (THF, CH_2Cl_2, $CHCl_3$, toluene) and was therefore easily characterized by NMR, UV/Vis and FTIR spectroscopies. The molecular weight (M_w) of **15** could not be determined by analytical SEC using the calibration curve of linear polystyrene (PS) as standard. Actually, as previously reported by Kraus and Müllen for fullerene-containing polymers,[44] this analysis revealed lower than expected molecular weights. This phenomenon is most probably caused by π-π interactions between the fullerene subunits and the phenyl moieties of the polystyrene stationary phase, leading to an increase of the elution volume with a corresponding decrease in the molecular weights. For this reason, polymer **15** was characterized by analytical SEC coupled with a light scattering detector, allowing the determination of an absolute molecular weight for **15** independently of a calibration curve. A value of $M_w = 59\,000$ g mol^{-1} (polydispersity: $M_w/M_n = 1.1$) was thus obtained for **15**, corresponding to an average polymerization degree of 25.

Owing to its high fullerene content and excellent solubility in common organic solvents, polyester **15** is an interesting polymeric acceptor for the preparation of all-polymer solar cells. In order to test its potential for such applications, photovoltaic cells have been prepared with blends of **15** and MDMO–PPV (Fig. 8). Thus, a chloroform solution of MDMO–PPV and **15** (1 : 5 by weight) has been spin coated on top of a poly(ethylenedioxythiophene)–poly(styrene sulfonate) (PEDOT–PSS, Baytrron P) covered indium–tin oxide (ITO). The thickness of the active layer determined *via* the surface profiler is about 100 nm. Two different cathode configurations were applied on top of the active material. In the first series 15 nm of calcium were evaporated on the polymer composition. Subsequently, in order to inhibit the oxidization of calcium, 200 nm of aluminum were evaporated on top of the calcium. In the second series, 0.7 nm lithium fluoride and 100 nm aluminum were evaporated successively. Calcium as well as lithium fluoride should allow a better contact to the organic layer than aluminum alone. The current-voltage (*I–V*) characteristics of both devices in the dark and under illumination (standard AM1.5 conditions) are depicted in Fig. 9. Under light, both devices show clear photovoltaic behavior. Cells with Ca/Al as cathode showed a short circuit current (I_{sc}) of 0.7 μA cm^{-2}, an open circuit voltage (V_{oc}) of 0.33 V and a fill factor (FF) of 0.37. Using the LiF/Al cathode resulted in an I_{sc} of 0.7 μA cm^{-2}, a V_{oc} of 0.36 V and a FF of 0.36. Comparing the two devices, it is obvious that there are not any major differences between the two cathodes. The short circuit current and the open circuit voltage of the devices reported herein are low when compared to the optimized MDMO–PPV/PCBM photovoltaic cells. The latter observations might be ascribed to the low conductivity of the fullerene polymer due to the presence of the large solubilizing groups attached to the fullerene monomer. Effectively, these groups may inhibit the fullerene-fullerene interactions necessary for the charge transport. On the other hand, it is also well-known that the solvent used for the spin coating of the active layer as well as the fullerene : PPV weight ratio of this film have a dramatic influence on the performances of the devices.[36] Therefore, further improvements can be expected by optimizing the processing of the fullerene-functionalized polymer/MDMO–PPV active layer.

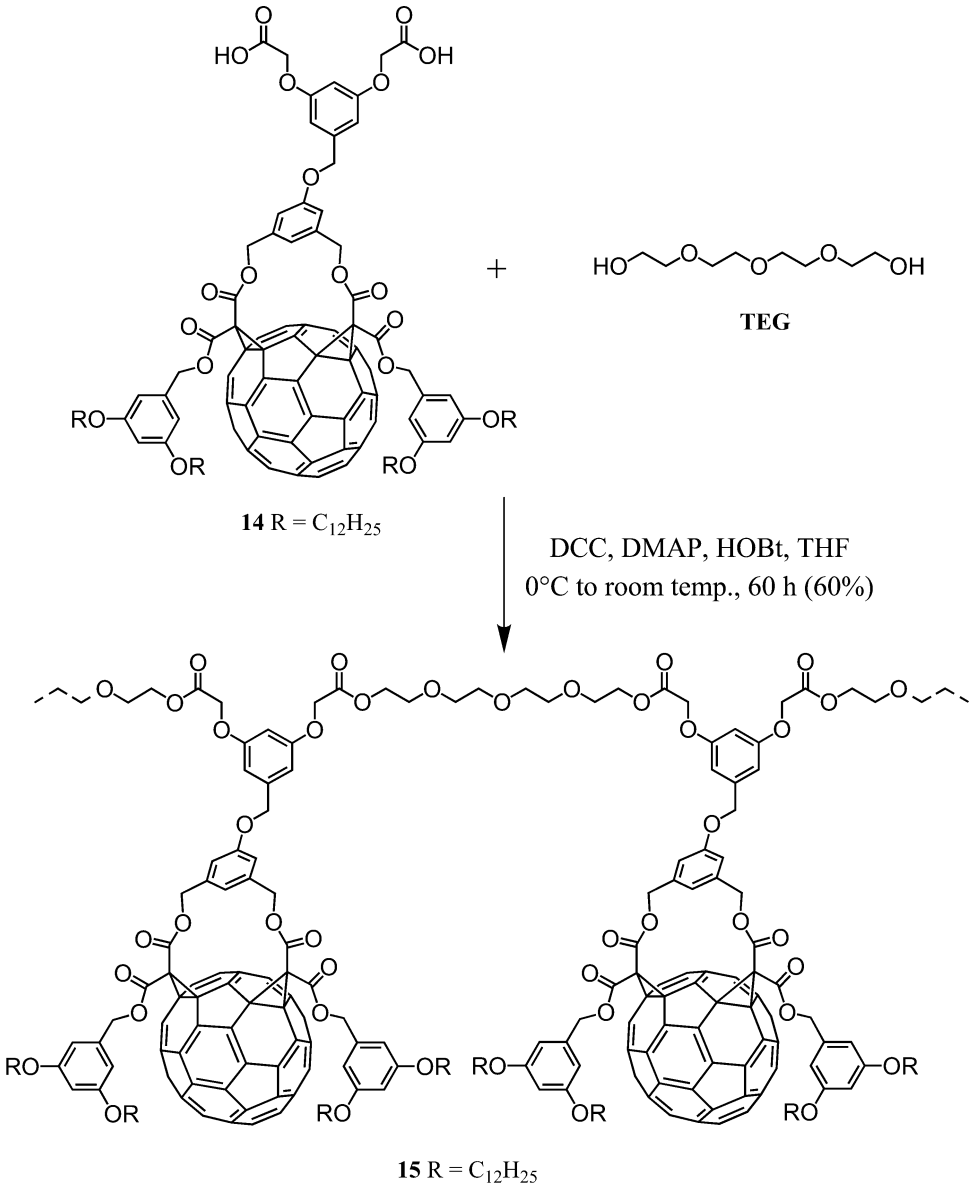

14 R = $C_{12}H_{25}$

15 R = $C_{12}H_{25}$

Scheme 1 Preparation of polymer **15**.

The performances of bulk heterojunction devices obtained from π-conjugated polymers and C_{60} derivatives are very sensitive to the morphology of the blend.[36] Ideally (to ensure efficient exciton dissociation), an acceptor species should be within the exciton diffusion range of any donor species and *vice versa*. Moreover, both the donor and the acceptor phases should form a bicontinuous microphase separated network to allow bipolar charge transport. However, the donor and acceptor molecules are usually incompatible and tend to undergo uncontrolled macrophase separation. In particular, phase separation and clustering of the fullerene can occur due to the operational heat through illumination, thus reducing the effective donor-acceptor interfacial area and the efficiency of the devices.[36] In order to prevent such undesirable effects, we have proposed that the bicontinuous network could be simply obtained by chemically linking a hole-conducting moiety to the electron-conducting fullerene subunit.[45] Based on these considerations, we have prepared compound **16** in which an oligophenylenevinylene (OPV) moiety is covalently linked to the fullerene sphere (Fig. 10). The C_{60}–OPV hybrid compound **16** has been incorporated in a photovoltaic cell constructed by spin casting the compound on a glass substrate covered with indium-tin oxide (ITO) and depositing an aluminum film on top. In such a device configuration, the compound is not only able to generate electrons and holes under light irradiation, but it also provides pathways for their subsequent collection at opposite electrodes, and a photocurrent is obtained.[45] The current-voltage characteristics of the ITO/**16**/Al device in the dark and under illumination, at $\lambda = 400$ nm with an intensity of 12 mW cm^{-2}, are depicted in Fig. 10. Forward bias is defined as the positive voltage applied to the ITO electrode. It is known that C_{60} can form "quasi-ohmic" contacts with Al and ITO electrodes. Therefore, the relatively high absolute value of the dark current, especially in reverse bias (Fig. 10), may be attributed to a continuous phase of C_{60} between the electrodes. Under illumination, the short circuit current density and the open circuit voltage are about 10 μA cm^{-2} and 0.46 V, respectively. The photosensitivity of this device at zero bias is about 0.8 mA W and the fill factor is equal to 0.3.

Even if the performances of the photovoltaic devices using an active layer constituted by a thin film of compound **16** are quite modest (the monochromatic power conversion efficiency of the ITO/**16**/Al device is equal to 0.01%), our study was the first demonstration that a bicontinuous network for plastic solar cells can be obtained by chemically linking a hole-conducting moiety to an electron-conducting fullerene subunit

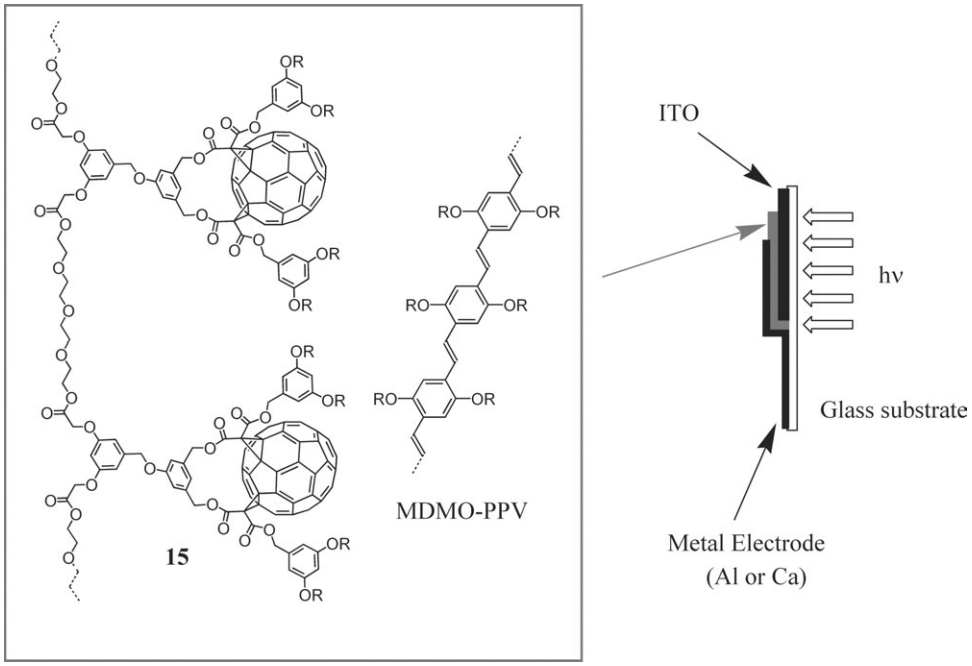

Fig. 8 Schematic representation of the photovoltaic device prepared from **15** and MDMO–PPV.

and it validated the proposed concept. At this stage, the challenge was to understand why the efficiencies of our first devices were so low. A first answer came from the photophysical investigations of C_{60}–OPV hybrid compounds.[46–48] Effectively, these studies revealed that in fluid solution (polar and apolar), an efficient singlet-singlet OPV → C_{60} photoinduced energy transfer occurs whereas electron transfer, if any, is a minor process (Fig. 11). Indeed, the efficiencies of the photovoltaic devices are low as a consequence of the prevalence of energy transfer *vs.* electron transfer, thus the main part of the light energy absorbed by the OPV fragment is promptly conveyed to the fullerene lowest singlet excited state, in analogy with the behavior in fluid solution.[48] In turn, the fullerene lowest singlet and triplet excited states cannot lead to charge separation, due to their low energy content (Fig. 11), thus electron-hole pairs can no longer be generated. Therefore, only a small part of the absorbed light is able to contribute effectively to the photocurrent.

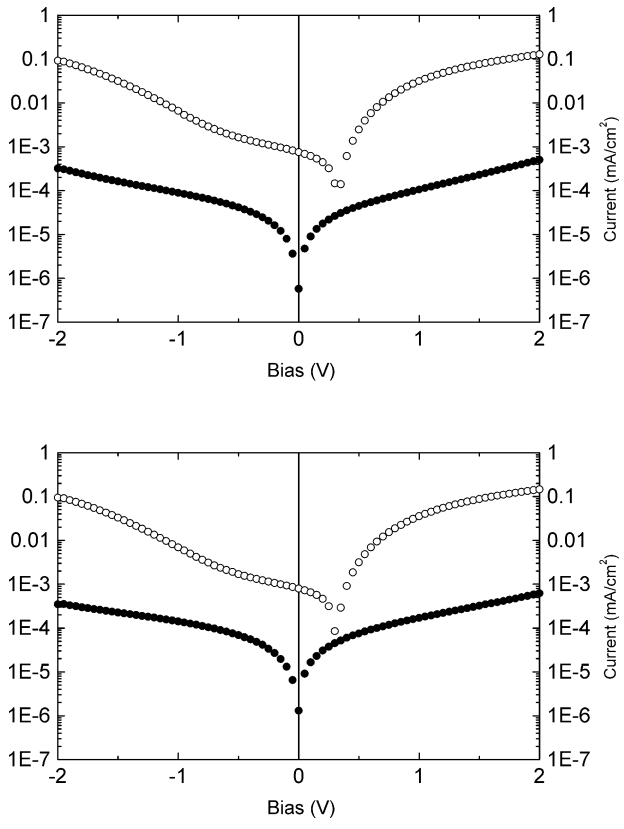

Fig. 9 Current-voltage (I–V) characteristics in the dark (filled circles) and under illumination (open circles) of the MDMO–PPV/**15** devices with the LiF/Al cathode (top) and the Ca/Al cathode (bottom).

As part of this study, we have also prepared compound **17** bearing an OPV tetrameric unit (Fig. 12).[48] Indeed, this compound is the higher homolog of the C_{60}–OPV derivative **16**. The current-voltage characteristics of the ITO/**17**/Al device in the dark and under illumination, at $\lambda = 400$ nm with an intensity of 12 mW cm^{-2}, are depicted in Fig. 12. Similarly to the ITO/**16**/Al device, the ITO/**17**/Al one shows almost symmetrical *I–V* characteristics in the dark. The photovoltaic characteristics of the ITO/**17**/Al device at zero bias are quite similar to those of the one obtained from **16**. An increase in the photosensitivity (2.2 mA W) occurs with a slight increase in the open circuit voltage (0.52 V). As discussed for compound **16**, the low efficiency results from the low contribution of the photoinduced electron transfer from the OPV moiety excited state to the C_{60} sphere as evidenced in solution by the photophysical investigations.[48] However, compared to **16**, the higher homolog, **17**, has a stronger absorption in the visible range and the photoinduced electron transfer becomes slightly easier since the donating ability of the longer OPV moiety is increased. For these reasons, the performance characteristics of the ITO/**17**/Al device (monochromatic power conversion efficiency of 0.03%) are significantly improved when compared to the ITO/**16**/Al one (monochromatic power conversion efficiency of 0.01%). This latest example shows clearly the advantage of our molecular approach allowing an understanding of structure-activity relationships.

Related fullerene derivatives in which an OPV subunit is attached to C_{60} through a pyrrolidine (**18**) or a pyrazoline (**19**) ring have also been reported (Chart 5).[49,50] The excited state properties of **18** and **19** have been investigated in solution. For compound **18**, quantitative OPV → C_{60} photoinduced singlet-singlet energy transfer has been evidenced in CH_2Cl_2. In the case of **19**, the excited state properties are more complex due to the electron-donating ability of the pyrazoline ring. As ob-

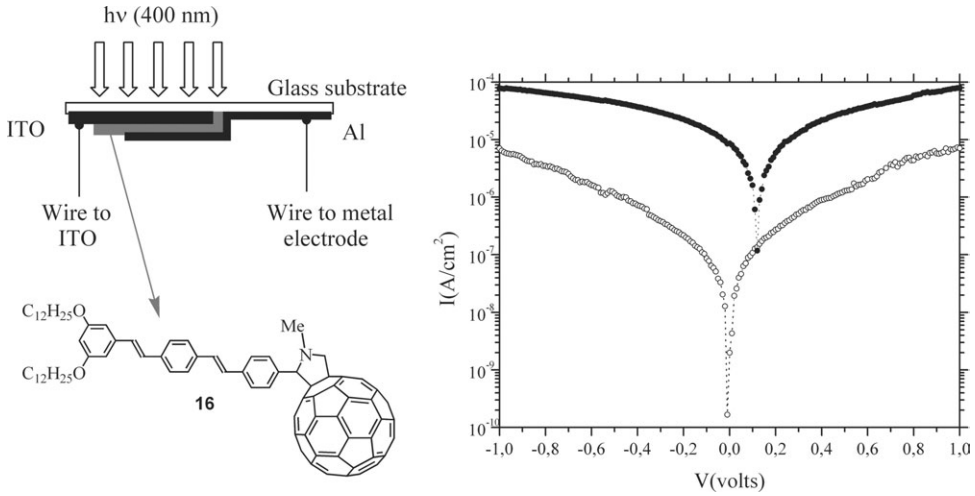

Fig. 10 Schematic structure of the ITO/**16**/Al device and current-voltage characteristics in the dark and under illumination, at $\lambda = 400$ nm with an intensity of 12 mW cm^{-2}.

served for **18**, quantitative OPV → C_{60} photoinduced singlet-singlet energy transfer occurs in **19** in CH_2Cl_2. However, in this case, the initial energy transfer event is followed by an efficient electron transfer from the N lone pair of the pyrazoline ring to the fullerene moiety.

Compounds **18** and **19** have been tested as active materials in photovoltaic devices. Each C_{60}–OPV conjugate has been sandwiched between PEDOT–PSS covered ITO and aluminum electrodes. The current-voltage curves of both devices have been recorded in the dark and under illumination.[49] In the dark, the current is found to be higher by at least two orders of magnitude for the ITO/PEDOT–PSS/**18**/Al device when compared to the ITO/PEDOT–PSS/**19**/Al one. The latter observation is likely due to better charge transport properties of the thin films prepared from compound **18**. In the case of **19**, the lower conductivity maybe ascribed to the presence of the pyrazoline N atom, which is able to act as a trap due to its electron-donating ability as evidenced by the photophysical studies. Under illumination, both devices show a clear photovoltaic behavior. As discussed for **16** and **17**, the monochromatic power conversion efficiency of the devices prepared from **18** are rather poor due to the low contribution of photoinduced electron transfer from the OPV moiety to the fullerene subunit since energy transfer remains the main deactivation pathway. Surprisingly, the performances of the devices obtained with **19** are not improved, even if efficient electron transfer has been evidenced for this compound. Actually, it seems that the charge separation involving the fullerene moiety and the pyrazoline N atom is not able to contribute to the photocurrent production since it does not involve the hole-conducting moiety (the OPV unit). In other words, only the photoinduced electron transfer from the OPV unit to the fullerene moiety is efficient for the photovoltaic effect. Since the latter is a minor deactivation pathway, only a small part of the absorbed light is able to contribute effectively to the photocurrent.

Recently, we have described the preparation of photovoltaic devices from the fullerene-oligophenyleneethynylene (OPE) conjugates **20**–**23** (Chart 6).[51,52] Each C_{60}–OPE conjugate has been sandwiched between PEDOT–PSS covered ITO and aluminum electrodes. The current-voltage characteristics of all the devices have been determined in the dark and under illumination (400 nm, 1 mW cm^{-2});[51] the results are summarized in Table 1.

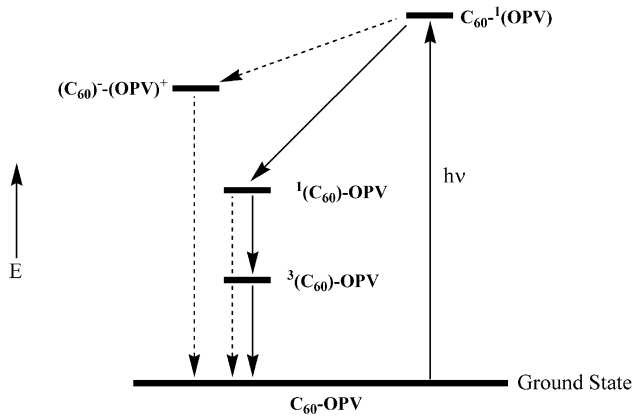

Fig. 11 Energy-level diagram describing the excited state deactivation pathways and the intercomponent processes for the C_{60}–OPV hybrid compound **16**.

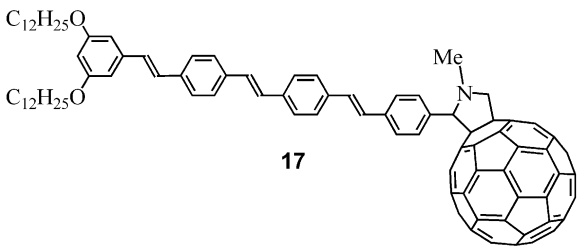

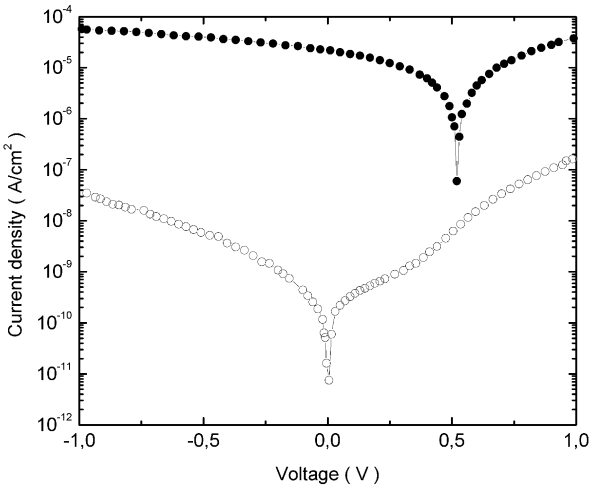

Fig. 12 Structure of compound **17** and current-voltage characteristics of the ITO/**17**/Al device in the dark and under illumination, at $\lambda =$ 400 nm with an intensity of 12 mW cm^{-2}.

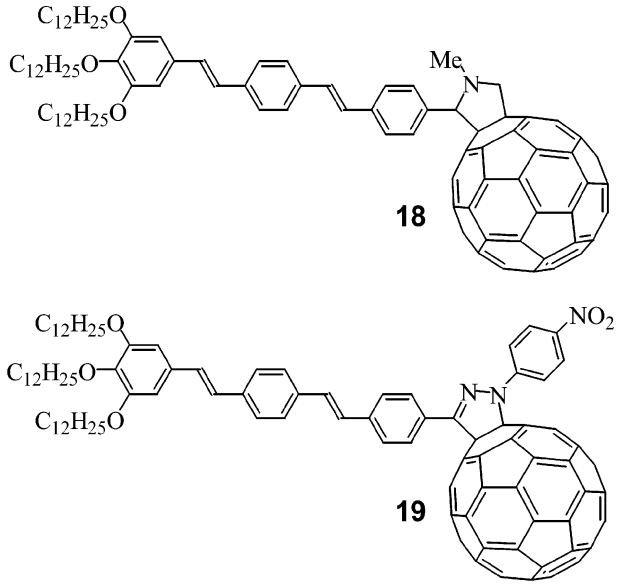

Chart 5 Compounds **18** and **19**.

In the dark, the current in reverse bias is higher by two orders of magnitude for the ITO/PEDOT–PSS/**20**/Al and ITO/PEDOT–PSS/**22**/Al devices when compared to the devices prepared from the corresponding higher homologues **21** and **23**. It is likely that the derivatives with the shortest OPE moieties exhibit better charge transport properties as their intrinsic fullerene : OPE weight ratio is higher. Under light, all the devices show clear photovoltaic behavior. Interestingly, the performances of the devices prepared from the *N*,*N*-dialkylaniline terminated derivatives **22** and **23** are significantly improved when compared to those obtained with **20** and **21**. This is also clearly shown by plotting the sensitivity as a function of the wavelength for all the devices: a higher sensitivity has been observed over the whole spectral range for the solar cells prepared from **22** and **23**. The latter observation can be related to the differences seen in their first oxidation potentials. Effectively, due to the increased donating ability of the OPE moiety in **22** and **23** as compared to **20** and **21**, the energy level of their charge-separated states resulting from a photoinduced electron transfer is significantly lower in energy. Therefore, the thermodynamic driving force is more favorable; thus, electron transfer, which is one of the key steps for photocurrent production, must be more efficient for **22** and **23**. As a result, the power conversion efficiency of the devices is increased by one order of magnitude.

In order to improve our understanding of these photovoltaic cells, the charge mobility properties of thin films prepared from **20**–**23** have been investigated.[53] This study was particularly interesting since it revealed a direct relationship between the chemical structure, the charge carrier mobility and the photovoltaic characteristics. Compounds **20**–**23** have been incorporated in field-effect transistors (FET's) to derive a value for the mobility of the charge carriers; the values are given in Table 2.

The low hole carrier mobility is most likely due to a poor packing of the OPE chains. The electron mobility, which is in all cases higher than the hole mobility, is very sensitive to the intrinsic C_{60} : OPE mass ratio. A decrease in mobility is clearly observed when this ratio decreases, as seen by going from **20** to **21** and from **22** to **23**. Surprisingly, the electron mobility is found to be almost one order of magnitude higher for **22** and **23** when compared to the corresponding homologs **20** and **21** lacking the *N*,*N*-dialkylaniline group. Therefore, the electron mobility is sensitive to the donating ability of the oligomer. In addition, the increase of polarity within the organic layer resulting from the presence of the amine functions might also play an important role.

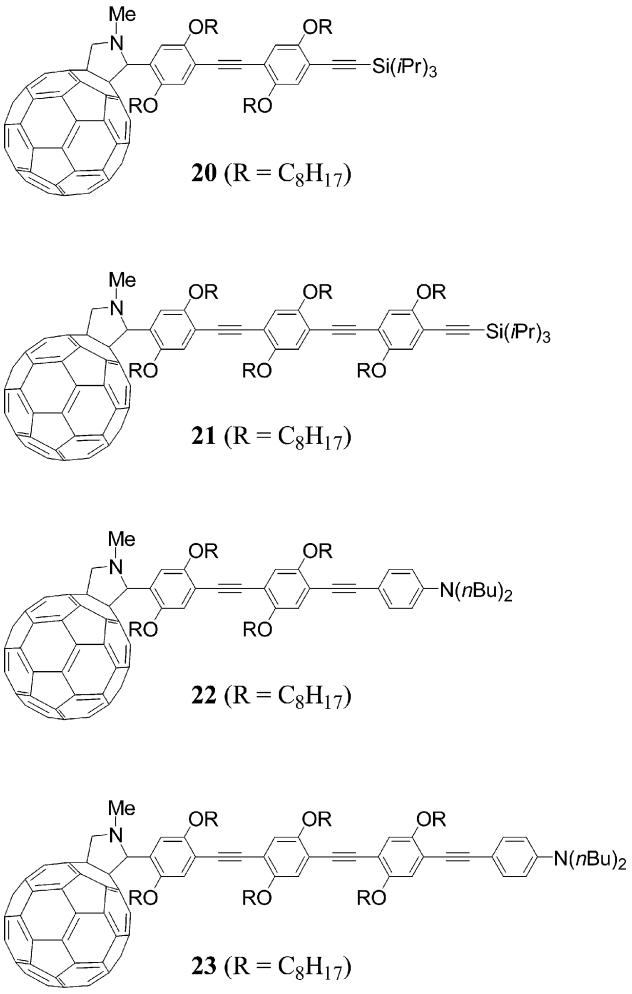

Chart 6 C_{60}–OPE derivatives **20**–**23**.

As seen in Table 1, the performance of the photovoltaic cells prepared from **20**–**23** is rather limited. Nevertheless, it is clear that the low mobility is an important limiting factor. Indeed, with the highest average charge carrier mobility, compound **22** exhibits also the highest short circuit current and the highest overall energy conversion efficiency. When compared to the photovoltaic cells obtained from **20** and **21**, the energy conversion efficiency and the short circuit current are increased in the devices prepared from **22** and **23**. This can be clearly related to the increased electron mobility observed for the *N*,*N*-dialkylaniline terminated derivatives. The improved donating ability of the oligomer in these latter cases certainly also facilitates the photoinduced electron transfer leading to the observed results. However, the slight increase of the hole mobility for compound **23** due to an increased oligomer length with respect to **22** cannot compensate for the decreased electron mobility due to its decreased C_{60} : OPE mass ratio. This is reflected in a lower η_e and I_{sc} for the ITO/PEDOT–PSS/**23**/Al device with respect to the ITO/PEDOT–PSS/**22**/Al cell. Similar considerations for the electron mobility changes for compounds **20** and **21** can be made, reflected in the I_{sc} result. The large difference in the efficiency in this case is mainly caused by the change of the open circuit voltage from 0.22 V for **20** to 0.58 V for **21**. In summary, a structure-activity relationship has clearly been established for this series of compounds. As far as the mobility properties are concerned, an increase in the oligomer chain length leads to a substantial increase of the mobility of positive charge carriers, but at the same time reduces the intrinsic C_{60} : OPE mass ratio in the hybrid molecules, thus decreasing the electron mobility. Nevertheless, improved donating ability of the oligomer facilitates the injec-

Table 1 Summary of the results concerning the photovoltaic measurements for the devices prepared from compounds **20–23**

Compound	V_{OC}/V	$I_{SC}/10^{-7} \cdot A\ cm^{-2}$	FF[a]	% T[b]	$S_{400}/10^{-4} \cdot A\ W^{-1}$	% $\eta_{e\ 400}/10^{-3}$[a]
20	0.22	2.05	0.27	55	2.41	1.2
21	0.58	2.04	0.22	27	1.81	2.6
22	0.54	11.6	0.32	22	14.6	20
23	0.59	10.6	0.29	39	10.1	18

[a] The calculation of the overall energy conversion efficiency η_e, has been done using the equation $\eta_{e} = V_{OC} \cdot I_{SC} \cdot FF/P_{INC}$, where V_{OC}, I_{SC}, FFand P_{INC} are the open circuit potential, short circuit current, filling factor and incident light power, respectively. The filling factor is given by $FF = (V_{MAX} \cdot I_{MAX})/(V_{OC} \cdot I_{SC})$ where V_{MAX} and I_{MAX} are voltage and current, respectively, at the point of maximum power output. Standard intensity of light was 1 mW cm^{-2}. [b] T = transmission (corrected on glass, ITO and PEDOT–PSS).

Table 2 Mobility values for the electrons and holes for compounds **20–23** obtained from measurements on field-effect transistors in the saturation regime

Compound	Electron mobility/ $10^{-7} \cdot cm^2\ V^{-1}\ s^{-1}$	Hole mobility/ $10^{-8} \cdot cm^2\ V^{-1}\ s^{-1}$
20	4.17	1.44
21	1.31	6.60
22	39.3	6.24
23	7.00	9.17

tion of negative charges, leading to a higher electron mobility and better solar cell performance. The compounds having the highest average charge carrier mobility exhibit the highest short circuit current and the most efficient energy conversion.

Following the preparation of the first photovoltaic devices from C_{60}–OPV and C_{60}–OPE conjugates, a great deal of attention has been devoted to C_{60} arrays substituted with π-conjugated oligomers[54] such as oligonaphthylenevinylene,[55] oligothiophenes,[56] and related systems.[57] Whereas the photophysical properties of these C_{60}–(π-conjugated oligomer) dyads have been extensively studied, only a few of them have been tested as the active layer of photovoltaic cells.[54–57] The highest power conversion efficiencies (0.2 to 0.4%) have been reported for hybrid compounds combining C_{60} with oligothiophene or azothiophene.[56,57] The generation of high photocurrents is ascribable to very efficient photoinduced charge separation.

Conclusion and perspectives

Our recent progress in the chemistry of C_{60} has allowed us to prepare a large variety of fullerene derivatives for various applications in materials science. In the first part of this paper, we have shown some of the fundamental architectural requirements needed for the design of amphiphilic fullerene derivatives capable of forming stable Langmuir films. The encapsulation of C_{60} in a cyclic addend surrounded by long alkyl chains, cholesterol subunits or dendritic branches is an efficient strategy to prevent the irreversible aggregation resulting from the strong fullerene-fullerene interactions usually observed for amphiphilic C_{60} derivatives at the air–water interface. These derivative have also been successfully incorporated in Langmuir–Blodgett films. In the second part, we have described water-soluble C_{60} derivatives, fullerene-functionalized dendrimers and fullerene-rich polymers. These compounds are easy to process owing their high solubility and/or film forming capabilities. Thus, the water-soluble derivative and the fullerodendrimers have been easily incorporated in mesoporous silica glasses and preliminary measurements on the resulting doped samples have revealed efficient optical limiting properties. On the other hand, the fullerene-containing polyesters have been used for the preparation of all-polymer donor-acceptor bulk heterojunction photovoltaic cells. Finally, our recent developments on organic photovoltaic cells using covalently linked fullerene–(π-conjugated oligomer) ensembles as the active layer have been summarized. This molecular approach appears to be particularly interesting since the bicontinuous donor-acceptor network obtained by chemically linking the hole-conducting moiety to the electron-conducting fullerene subunit prevents any problems arising from bad contacts at the junction, as observed for polymer/C_{60} blends. Furthermore, the behavior of a unique molecule in a photovoltaic cell and the study of its electronic properties mean that one can easily obtain the structure-activity relationships leading to a better understanding of the photovoltaic conversion. The molecular approach to the photovoltaic conversion is not only an interesting model for a better understanding of the devices using bulk heterojunction materials but it appears also as an excellent alternative to the polymeric approach. Effectively, the photosensivity and the energy conversion efficiency obtained with devices prepared with fullerene–(π-conjugated oligomer) dyads capable of achieving efficient and very fast photoinduced charge separation are quite promising. Furthermore, this new synthetic approach also offers great versatility for design tuning of the photovoltaic system. However, for commercial use, the efficiency of the organic photodiodes has to be improved dramatically. For these purposes, new hybrid compounds with a stronger absorption in the visible range and a better stability towards light are needed. In addition, the performances of the molecular photovoltaic cells are mainly limited by their low conductivity. Therefore, a critical point appears to be the orientation of the molecules within the thin film to improve the conductivity. In this respect, the use of liquid-crystalline C_{60}–(π-conjugated oligomer) conjugates could be of particular interest since such materials would spontaneously form ordered assemblies that could then be oriented and lead to high-performance thin films.[58]

Acknowledgements

This work was supported by the CNRS, the French Ministry of Research (ACI Jeunes Chercheurs 2000), ECODEV (CNRS-ADEME, research program on photovoltaic conversion), the Région Alsace and the EU (RTN "FAMOUS", HPRN-CT-2002-00171). I would like to warmly thank all my co-workers for their outstanding contributions, their names are cited in the references. This multidisciplinary research was only possible thanks to collaborations with colleagues all around the world: T. Aernouts (IMEC, Leuven, Belgium), N. Armaroli (CNR, Bologna, Italy), P. Ceroni (Università di Bologna, Italy), R. Deschenaux (Université de Neuchâtel, Switzerland), L. Echegoyen (Clemson University, USA), J.-L. Gallani (IPCMS, Strasbourg, France), M. Gross (Université Louis Pasteur, Strasbourg, France), G. Hadziioannou (ECPM, Strasbourg, France), B. Hönerlage (IPCMS, Strasbourg, France), F. Langa (Universidad de Castilla-La Mancha, Toledo, Spain), R. Lévy (IPCMS, Strasbourg, France), P. Masson (IPCMS, Strasbourg, France), A. Rameau (ICS, Strasbourg, France), J.-L. Rehspringer (IPCMS, Strasbourg, France), S. Setayesh (Philips Electronics, Eindhoven, The Netherlands) and N. Solladié (Université Louis

Pasteur, Strasbourg, France). I would like to thank all of them for their enthusiasm, support and contributions.

References

1 W. Krätschmer, L. D. Lamb, K. Fostiropoulos and D. R. Huffman, *Nature (London)*, 1990, **347**, 354.
2 L. Echegoyen and L. E. Echegoyen, *Acc. Chem. Res.*, 1998, **31**, 593.
3 (*a*) R. C. Haddon, A. F. Hebard, M. J. Rosseinski, D. W. Murphy, S. J. Duclos, K. B. Lyons, B. Miller, J. M. Zahurak, R. Tycko, G. Dabbagh and F. A. Thiel, *Nature (London)*, 1991, **350**, 320; (*b*) K. Holczer, O. Klein, S.-M. Huang, R. B. Kaner, K.-J. Fu, R. L. Whetten and F. Diederich, *Science*, 1991, **252**, 1154.
4 L. W. Tutt and A. Krost, *Nature (London)*, 1992, **356**, 225.
5 R. S. Ruoff, D. S. Tse, R. Malhotra and D. C. Lorents, *J. Phys. Chem.*, 1993, **97**, 3379.
6 (*a*) A. Hirsch, *The Chemistry of the Fullerenes*, Thieme, Stuttgart, 1994; (*b*) F. Diederich, L. Isaacs and D. Philp, *Chem. Soc. Rev.*, 1994, **23**, 243; (*c*) F. Diederich and C. Thilgen, *Science*, 1996, **271**, 317; (*d*) M. Prato and M. Maggini, *Acc. Chem. Res.*, 1998, **31**, 519; (*e*) F. Diederich and R. Kessinger, *Acc. Chem. Res.*, 1999, **32**, 537; (*f*) J.-F. Nierengarten, *Chem.-Eur. J.*, 2000, **6**, 3667.
7 (*a*) C. A. Mirkin and W. B. Caldwell, *Tetrahedron*, 1996, **52**, 5113 and references therein; (*b*) L. Valli and D. M. Guldi, in *Fullerenes: from Synthesis to Optoelectronic Properties*, eds. D. M. Guldi and N. Martin, Kluwer Academic Publishers, Dordrecht, 2002, p. 327.
8 For examples, see: (*a*) Y. S. Obeng and A. J. Bard, *J. Am. Chem. Soc.*, 1991, **113**, 6279; (*b*) T. Nakamura, H. Tachibana, M. Yamura, M. Matsumoto, R. Azumi, M. Tanaka and Y. Kawabata, *Langmuir*, 1992, **8**, 4; (*c*) P. Wang, M. Shamsuzzoha, X.-L. Wu, W.-J. Lee and R. M. Metzger, *J. Phys. Chem.*, 1992, **96**, 9025.
9 (*a*) J. A. Milliken, D. D. Dominguez, H. H. Nelson and W. R. Barger, *Chem. Mater.*, 1992, **4**, 252; (*b*) C. Ewins and B. Steward, *J. Chem. Soc., Faraday Trans.*, 1994, **90**, 969; (*c*) S. S. Shiratori, M. Shimizu and K. Ikezaki, *Thin Solid Films*, 1998, **327–329**, 655.
10 F. Diederich, J. Effing, U. Jonas, L. Jullien, T. Plesnivy, H. Ringsdorf, C. Thilgen and D. Weinstein, *Angew. Chem., Int. Ed Engl.*, 1992, **31**, 1599.
11 (*a*) P. L. Nostro, A. Casnati, L. Bossoletti, L. Dei and P. Baglioni, *Colloids Surf., A*, 1996, **116**, 203; (*b*) Z. I. Kazantseva, N. V. Lavrik, A. V. Nabok, O. P. Dimitriev, B. A. Nesterenko, V. I. Kalchenko, S. V. Vysotsky, L. N. Markovskiy and A. A. Marchenko, *Supramol. Sci.*, 1997, **4**, 341; (*c*) L. Dei, P. L. Nostro, G. Capuzzi and P. Baglioni, *Langmuir*, 1998, **14**, 4143.
12 U. Jonas, F. Cardullo, P. Belik, F. Diederich, A. Gügel, E. Harth, A. Herrmann, L. Isaacs, K. Müllen, H. Ringsdorf, C. Thilgen, P. Uhlmann, A. Vasella, C. A. A. Waldraff and M. Walter, *Chem.-Eur. J.*, 1995, **1**, 243.
13 For examples, see: (*a*) L. M. Goldenberg, G. Williams, M. R. Bryce, A. P. Monkman, M. C. Petty, A. Hirsch and A. Soi, *J. Chem. Soc., Chem. Commun*1993, 1310; (*b*) C. J. Hawker, P. M. Saville and J. W. White, *J. Org. Chem.*, 1994, **59**, 3503; (*c*) M. Maggini, L. Pasimeni, M. Prato, G. Scorrano and L. Valli, *Langmuir*, 1994, **10**, 4164; (*d*) S. Ravaine, F. Le Pecq, C. Mingotaud, P. Delhaes, J. C. Hummelen, F. Wudl and L. K. Patterson, *J. Phys. Chem.*, 1995, **99**, 9551; (*e*) P. Wang, B. Chen, R. M. Metzger, T. Da Ros and M. Prato, *J. Mater. Chem.*, 1997, **7**, 2397; (*f*) D. M. Guldi, M. Maggini, S. Mondini, F. Guérin and J. H. Fendler, *Langmuir*, 2000, **16**, 1311; (*g*) S. Zhang, L. Gan and C. Huang, *Chem. Phys. Lett.*, 2000, **331**, 143; (*h*) M. Carano, P. Ceroni, F. Paolucci, S. Roffia, T. Da Ros, M. Prato, M. I. Sluch, C. Pearson, M. C. Petty and M. R. Bryce, *J. Mater. Chem.*, 2000, **10**, 269.
14 J.-F. Nierengarten, C. Schall, J.-F. Nicoud, B. Heinrich and D. Guillon, *Tetrahedron Lett.*, 1998, **39**, 5747.
15 J.-F. Nierengarten and J.-F. Nicoud, *Tetrahedron Lett.*, 1997, **38**, 7737.
16 D. Felder, J.-L. Gallani, D. Guillon, B. Heinrich, J.-F. Nicoud and J.-F. Nierengarten, *Angew. Chem., Int. Ed.*, 2000, **39**, 201.
17 D. Felder, M. Gutiérrez Nava, M. del Pilar Carreon, J.-F. Eckert, M. Luccisano, C. Schall, P. Masson, J.-L. Gallani, B. Heinrich, D. Guillon and J.-F. Nierengarten, *Helv. Chim. Acta*, 2002, **85**, 288.
18 D. Felder, M. del Pilar Carreon, J.-L. Gallani, D. Guillon, J.-F. Nierengarten, T. Chuard and R. Deschenaux, *Helv. Chim. Acta*, 2001, **84**, 1119.
19 F. Cardulo, F. Diederich, L. Echegoyen, T. Habicher, N. Jayaraman, R. M. Leblanc, J. F. Stoddart and S. Wang, *Langmuir*, 1998, **14**, 1955.
20 J.-F. Nierengarten, J.-F. Eckert, Y. Rio, M. P. Carreon, J.-L. Gallani and D. Guillon, *J. Am. Chem. Soc.*, 2001, **123**, 9743.
21 S. Zhang, Y. Rio, F. Cardinali, C. Bourgogne, J.-L. Gallani and J.-F. Nierengarten, *J. Org. Chem.*, 2003, **68**, 9787.
22 J. Schell, D. Felder, J.-F. Nierengarten, J.-L. Rehspringer, R. Lévy and B. Hönerlage, *J. Sol-gel Sci. Technol.*, 2001, **22**, 225.
23 (*a*) F. Henari, J. Callaghan, H. Stiel, W. Blau and D. J. Cardin, *Chem. Phys. Lett.*, 1992, **199**, 14; (*b*) D. G. McLean, R. L. Sutherland, M. C. Brant and D. M. Brandelik, *Opt. Lett.*, 1993, **18**, 858; (*c*) C. Li, L. Zhang, R. Wang, Y. L. Song and Y. Wang, *J. Opt. Soc. Am. B*, 1994, **11**, 1356; (*d*) S. Couris, E. Koudoumas, A. A. Ruth and S. Leach, *J. Phys. B*, 1995, **28**, 4537; (*e*) C. Li, J. H. Si, M. Yang, R. B. Wang and L. Zhang, *Phys. Rev. A*, 1995, **51**, 569.
24 (*a*) J. Schell, D. Brinkmann, D. Ohlmann, B. Hönerlage, R. Levy, M. Joucla, J.-L. Rehspringer, J. Serughetti and C. Bovier, *J. Chem. Phys.*, 1998, **108**, 8599; (*b*) J. Schell, D. Ohlmann, D. Brinkmann, R. Lévy, M. Joucla, J.-L. Rehspringer and B. Hönerlage, *J. Chem. Phys.*, 1999, **111**, 5929; (*c*) F. Bentivegna, M. Canva, P. Georges, A. Brun, F. Chaput, L. Malier and J.-P. Boilot, *Appl. Phys. Lett.*, 1993, **62**, 1721.
25 A. Krost, L. Tutt, M. B. Klein, T. K. Dougherty and W. E. Elias, *Opt. Lett.*, 1993, **18**, 334.
26 R. Gvishi, J. D. Bhawalkar, N. D. Kumar, G. Ruland, U. Narang, P. N. Prasad and B. A. Reinhardt, *Chem. Mater.*, 1995, **7**, 2199.
27 For examples, see: (*a*) R. Signorini, M. Zerbetto, M. Meneghetti, R. Bozio, M. Maggini, C. De Faveri, M. Prato and G. Scorrano, *Chem. Commun.*, 1996, 1891; (*b*) M. Maggini, C. De Faveri, G. Scorrano, M. Prato, G. Brusatin, M. Guglielmi, M. Meneghetti, R. Signorini and R. Bozio, *Chem.-Eur. J.*, 1999, **5**, 2501; (*c*) Y.-P. Sun, G. E. Lawson, J. E. Riggs, B. Ma, N. Wang and D. K. Moton, *J. Phys. Chem. A*, 1998, **102**, 5520.
28 D. Felder, D. Guillon, R. Lévy, A. Mathis, J.-F. Nicoud, J.-F. Nierengarten, J.-L. Rehspringer and J. Schell, *J. Mater. Chem.*, 2000, **10**, 887.
29 Y. Rio, J.-F. Nicoud, J.-L. Rehspringer and J.-F. Nierengarten, *Tetrahedron Lett.*, 2000, **41**, 10 207.
30 Y. Rio, G. Accorsi, H. Nierengarten, J.-L. Rehspringer, B. Hönerlage, G. Kopitkovas, A. Chugreev, A. Van Dorsselaer, N. Armaroli and J.-F. Nierengarten, *New J. Chem.*, 2002, **26**, 1146.
31 J.-F. Nierengarten, N. Armaroli, G. Accorsi, Y. Rio and J.-F. Eckert, *Chem.-Eur. J.*, 2003, **9**, 36.
32 J.-F. Nierengarten, *Top. Curr. Chem.*, 2003, **228**, 87.
33 Y. Rio, G. Accorsi, H. Nierengarten, C. Bourgogne, J.-M. Strub, A. Van Dorsselaer, N. Armaroli and J.-F. Nierengarten, *Tetrahedron*, 2003, **59**, 3833.
34 N. S. Sariciftci, L. Smilowitz, A. J. Heeger and F. Wudl, *Science*, 1992, **258**, 1474.
35 G. Yu, J. Gao, J. C. Hummelen, F. Wudl and A. J. Heeger, *Science*, 1995, **270**, 1789.
36 C. J. Brabec, N. S. Sariciftci and J. C. Hummelen, *Adv. Funct. Mater.*, 2001, **11**, 15 and references therein.
37 E. Shaheen, C. J. Brabec, N. S. Sariciftci, F. Pradinger, T. Fromherz and J. C. Hummelen, *Appl. Phys. Lett.*, 2001, **78**, 841.
38 M. Gutiérrez-Nava, S. Setayesh, A. Rameau, P. Masson and J.-F. Nierengarten, *New J. Chem.*, 2002, **26**, 1584.
39 M. Gutiérrez-Nava, P. Masson and J.-F. Nierengarten, *Tetrahedron Lett.*, 2003, **44**, 4487.
40 *Fullerene Polymers and Fullerene Polymer Composites*, eds. P. C. Eklund and A. M. Rao, Springer series in Materials Science, Vol. 38, Springer Verlag, Berlin, 2000.
41 For examples, see: (*a*) L. Y. Chiang, L. Y. Wang, S.-G. Tseng, J.-S. Wu and K.-H. Hsieh, *J. Chem. Soc., Chem. Commun.*, 1994, 2675; (*b*) S. Delpeux, F. Beguin, R. Benoit, R. Erre, N. Manolova and I. Rashkov, *Eur. Polym. J.*, 1998, **34**, 905; (*c*) Y. Ederlé and C. Mathis, *Macromol. Rapid Commun.*, 1998, **19**, 543; (*d*) Y. Chen, D. Yang, X. Yan, Z.-E. Huang, R. Cai, Y. Zhao and S. Chen, *Eur. Polym. J.*, 1998, **34**, 1755; (*e*) Y. Ederlé and C. Mathis, *Macromolecules*, 1999, **32**, 554.
42 For examples, see: (*a*) Y.-P. Sun, B. Liu and D. K. Moton, *Chem. Commun.*, 1996, 2699; (*b*) L. Dai, A. W. H. Mau and X. Zhang, *J. Mater. Chem.*, 1998, **8**, 325; (*c*) B. Liu, C. E. Bunker and Y.-P. Sun, *Chem. Commun.*, 1996, 1241; (*d*) K. E. Geckeler and A. Hirsch, *J. Am. Chem. Soc.*, 1993, **115**, 3850; (*e*) E. Cloutet, J.-L. Fillaut, D. Astruc and Y. Gnanou, *Macromolecules*, 1999, **32**, 1043; (*f*) X. D. Huang and S. H. Goh, *Macromolecules*, 2000, **33**, 8894.

43 For examples, see: (*a*) S. Shi, K. C. Khemani, Q. C. Li and F. Wudl, *J. Am. Chem. Soc.*, 1992, **114**, 10 656; (*b*) J. Li, T. Yoshizawa, M. Ikuta, M. Ozawa, K. Nakahara, T. Hasegawa, K. Kitazawa, M. Hayashi, K. Kinbara, M. Nohara and K. Saigo, *Chem. Lett.*, 1997, 1037; (*c*) M. Taki, S. Takigami, Y. Watanabe, Y. Nakamura and J. Nishimura, *Polym. J.*, 1997, **29**, 1020.

44 A. Kraus and K. Müllen, *Macromolecules*, 1999, **32**, 4214.

45 J.-F. Nierengarten, J.-F. Eckert, J.-F. Nicoud, L. Ouali, V. Krasnikov and G. Hadziioannou, *Chem. Commun.*, 1999, 617.

46 N. Armaroli, F. Barigelletti, P. Ceroni, J.-F. Eckert, J.-F. Nicoud and J.-F. Nierengarten, *Chem. Commun.*, 2000, 599.

47 N. Armaroli, F. Barigelletti, P. Ceroni, J.-F. Eckert and J.-F. Nierengarten, *Int. J. Photoenergy*, 2001, **3**, 33.

48 J.-F. Eckert, J.-F. Nicoud, J.-F. Nierengarten, S.-G. Liu, L. Echegoyen, F. Barigelletti, N. Armaroli, L. Ouali, V. Krasnikov and G. Hadziioannou, *J. Am. Chem. Soc.*, 2000, **122**, 7467.

49 N. Armaroli, G. Accorsi, J.-P. Gisselbrecht, M. Gross, V. Krasnikov, D. Tsamouras, G. Hadziioannou, M. J. Gomez-Escalonilla, F. Langa, J.-F. Eckert and J.-F. Nierengarten, *J. Mater. Chem.*, 2002, **12**, 2077.

50 M. J. Gomez-Escalonilla, F. Langa, J.-M. Rueff, L. Oswald and J.-F. Nierengarten, *Tetrahedron Lett.*, 2002, **43**, 7507.

51 T. Gu, D. Tsamouras, C. Melzer, V. Krasnikov, J.-P. Gisselbrecht, M. Gross, G. Hadziioannou and J.-F. Nierengarten, *Chem. Phys. Chem.*, 2002, **3**, 124.

52 T. Gu and J.-F. Nierengarten, *Tetrahedron Lett.*, 2001, **42**, 3175.

53 J.-F. Nierengarten, T. Gu, T. Aernouts, W. Geens, J. Poortmans, G. Hadziioannou and D. Tsamouras, *Appl. Phys. A*, 2004, **79**, 47.

54 E. Peeters, P. A. van Hal, J. Knol, C. J. Brabec, N. S. Sariciftci, J. C. Hummelen and R. A. J. Janssen, *J. Phys. Chem. B*, 2000, **104**, 10 174.

55 D. M. Guldi, C. Luo, A. Swartz, R. Gomez, J. L. Segura, N. Martin, C. Brabec and S. Sariciftci, *J. Org. Chem.*, 2002, **67**, 1141.

56 N. Negishi, K. Yamada, K. Takimiya, Y. Aso, T. Otsubo and Y. Harima, *Chem. Lett.*, 2003, 404.

57 M. Maggini, G. Possamai, E. Menna, G. Scorrano, N. Camaioni, G. Ridolfi, G. Casalbore-Miceli, L. Franco, M. Ruzzi and C. Corvaja, *Chem. Commun.*, 2002, 2028.

58 S. Campidelli, R. Deschenaux, J.-F. Eckert, D. Guillon and J.-F. Nierengarten, *Chem. Commun.*, 2002, 656.